Journal of Materials and Electronic Devices 1(2016) 11-15

JOURNAL OF MATERIALS AND ELECTRONIC DEVICES
FYTRONIX JMED
http://dergi-fytronix.com/

# Structural, morphological and optical properties of indium oxide film by sol gel spin coating

S. Ilican, M. Caglar, Y. Caglar
*Department of Physics, Faculty of Science, Anadolu University, Eskisehir, Turkey*

Indium oxide ($In_2O_3$) film has been deposited onto the glass substrates by the sol-gel spin coating method. The structural, morphological and optical properties of the film were investigated. In(III)Chloride, ethanol and hydrogen chloride (HCl) were used as a starting material, solvent and stabilizer, respectively. For investigation of crystal structure and orientation of the films, X-ray diffraction (XRD) patterns were used. The grain size of the film was calculated using the Scherrer formula. Using a spectrophotometer having an integrating sphere carried out the optical absorbance and transmittance measurements. The optical absorption studies revealed the transitions having the direct band gap. The optical parameters (the refractive index, extinction coefficient) were analyzed by using the reflectance and transmittance spectra. The refractive index dispersion curve shows that the $In_2O_3$ film obeys the single oscillator model.

*Keywords:* Indium Oxide, XRD, FESEM, optical constants, dispersion parameters.

*Submission date:01 December 2015*
*Acceptance date:23 April 2016*

*Corresponding author*: silican@anadolu.edu.tr

## 1. Introduction

Indium oxide ($In_2O_3$) is one of the n-type transparent wide band gap semiconductors (3.55–3.75 eV). $In_2O_3$ crystallizes in the bixbyite structure, with 40 atoms per primitive cell. Each indium atom is bonded to four O atoms and the latter are fourfold coordinated [1]. This material has been extensively used in electrochemical sensors [2], liquid crystal displays [3], photovoltaic cells [4], biosensing [5] and thin film transistor [6] because $In_2O_3$ has superior properties such as high visible wavelength transparency and electrical conductivity. It is often doped with tin (to produce ITO) in order to produce low resistivity and high mobility material and that being used in display devices for years ago [7-9].

$In_2O_3$ films have been widely used in glass coating applications, especially as transparent heating elements, and in the optoelectronic devices as transparent electrodes. Also, It is found its application as transparent heat mirror coating in buildings and cars, and due to their high reflectivity property in IR and a part of NIR spectrum, it is used in incandescent light bulbs to save the energy. However, indium oxide is still preferable than ITO because it has other potential applications such as an active layer in electronics and short wavelength optoelectronic devices. These films have been prepared by, sol gel [10], spray pyrolysis [11], pulse laser deposition (PLD) [12], flash evaporated [13]. Among many techniques that are used for preparing $In_2O_3$ films, sol–gel method has many advantages such as excellent compositional control, simplicity, homogeneity, lower crystallization temperature and low production costs. In the present work, our aim is to investigate structural, morphological and optical properties of $In_2O_3$ film so that this information would be helping the researchers toward applying these materials in optical devices and heterojunction solar cells.

## 2. Experimental details

$In_2O_3$ film was deposited by sol gel method spin coating technique onto glass substrates. In(III)Chloride, ethanol and hydrogen chloride were used as a starting material, solvent and stabilizer, respectively. The molar ratio of hydrogen chloride to In(III)Chloride was maintained at 1.0

and the concentration of In(III)Chloride was 0.005 M. The glass substrate was cleaned as chemically using ultrasonic cleaner. After the dropping of solution on the glass substrate, spin coater was rotated at 2500 rpm for 30 s. Then, following the spin coating depositing the film was dried at 300ºC for 10 min in a tube furnace. Each coating and drying procedures were repeated ten times. The film was annealed into a tube furnace in air at 550 ºC for 1 hour.

X-ray diffraction (XRD) pattern of the film was obtained by BRUKER D2 PHASER X-Ray Automatic Diffractometer at room temperature. ZEISS Ultraplus field emission scanning electron microscopy (FESEM) was used to investigate surface morphology. In the wavelength range from 190 to 900 nm, the optical transmittance and reflectance spectra of the film was performed by using SHIMADZU UV-VIS 2450 spectrophotometer with integrating sphere.

## 3. Results and discussion

### 3. 1. Structural properties of the $In_2O_3$ film

The XRD spectrum for the In2O3 film is shown in Fig. 1.

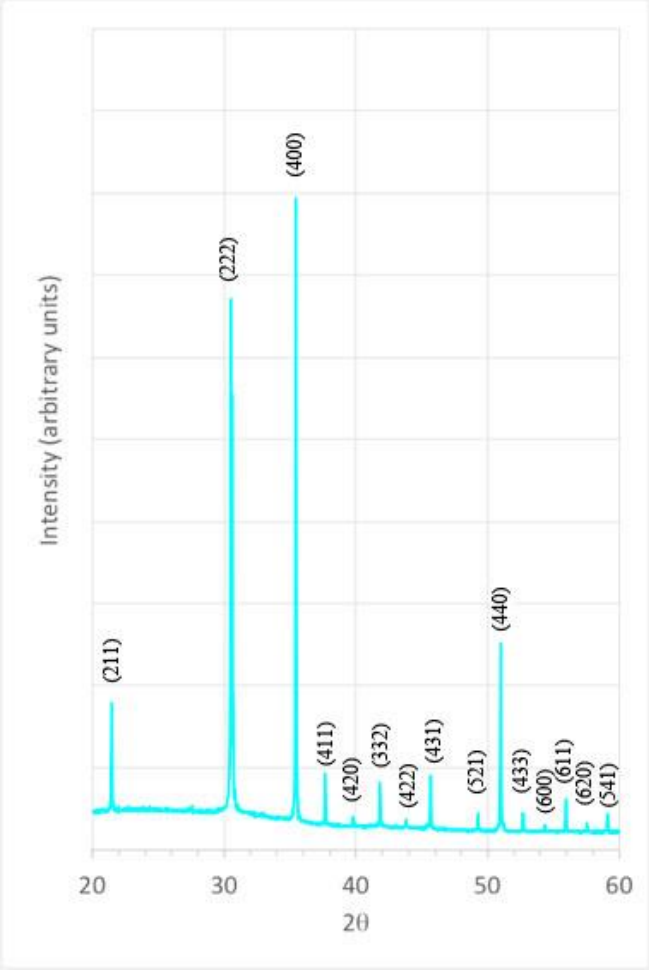


*Fig. 1. XRD spectra of the $In_2O_3$ film.*

It can be seen that $In_2O_3$ the film has polycrystalline structure. Similar XRD patterns were observed in the literature [14, 15]. Analyses of XRD data reveal the peaks corresponding to the (211), (222), (400), (332), (431), (440) and (622) planes of the cubic bixbyite structure crystal structure. All the peak positions are in good agreement with the JCPDS file card no. 06-0416 for $In_2O_3$. The angle of diffraction ($2\theta$), lattice spacing ($d$), $TC(hkl)$ values of the film are tabulated in Table 1.

*Table 1. Structural parameters of the $In_2O_3$ film*

| ***(h k l)*** | ***2θ*** | ***d (Å)*** | ***I/Io*** | ***TC (h k l)*** |
|---|---|---|---|---|
| (211) | 21.475 | 4.134 | 0.51 | 0.91 |
| **(222)** | **30.573** | **2.922** | **1.00** | **1.80** |
| (400) | 35.425 | 2.532 | 0.91 | 1.63 |
| (411) | 37.674 | 2.385 | 0.39 | 0.70 |
| (420) | 39.802 | 2.263 | 0.80 | 1.44 |
| (332) | 41.809 | 2.158 | 0.53 | 0.96 |
| (422) | 43.786 | 2.066 | 0.70 | 1.26 |
| (431) | 45.652 | 1.986 | 0.33 | 0.59 |
| (521) | 49.250 | 1.849 | 0.43 | 0.76 |
| (440) | 50.983 | 1.789 | 0.29 | 0.51 |
| (433) | 52.693 | 1.736 | 0.40 | 0.72 |
| (600) | 54.316 | 1.688 | 0.60 | 1.08 |
| (611) | 55.954 | 1.642 | 0.40 | 0.72 |
| (620) | 57.536 | 1.601 | 0.65 | 1.17 |
| (541) | 59.107 | 1.562 | 0.43 | 0.76 |

For the estimation of crystallite size ($D$) of the film Scherrer's equation [16] was used and in this calculation the data belongs to (222) reflection of $In_2O_3$ film was used and its value was obtained as 136nm.

The texture coefficient ($TC(hkl)$) that is used to determine preferential growth orientation is calculated is using the following relation [17]

$$TC(hkl) = \frac{{}^{I(hkl)}/_{I_{0(hkl)}}}{N^{-1}\sum {}^{I(hkl)}/_{I_{0(hkl)}}} \quad (1)$$

where $I(hkl)$ is the measured relative intensity of a plane ($hkl$), $I_o(hkl)$ is the standard intensity of the plane ($hkl$) taken from the JCPDS data, $N$ is the reflection number and $n$ is the number of diffraction peaks. The texture coefficient of the film was calculated for the main diffraction peaks and given in Table 1. It can be seen that the highest *TC(hkl)* value belongs to (222) plane of the film.

### 3. 2. Morphological properties of the $In_2O_3$ film

FESEM images that is taken at two different magnifications and that is obtained to investigate the surface morphology of $In_2O_3$ film are illustrated in figure 2.

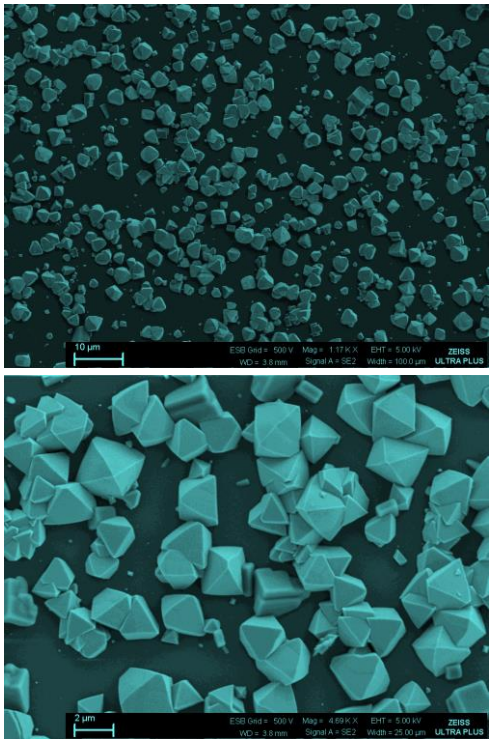

*Fig. 2. FESEM image of the $In_2O_3$ film.*

As seen in this Fig. 2, there are pyramid-shaped big crystals with an approximate size ranging between 7 and 10 μ on the surface of $In_2O_3$ film.

### 3.3. Optical properties of the $In_2O_3$ film

To get information on the optical properties of the $In_2O_3$ film, the optical transmittance and reflectance measurements were used in the wavelength range of 200–800nm (as shown in figure 3). As a reference, an uncoated glass substrate and a $BaSO_4$ were used, respectively before the transmittance and reflectance measurements. The average transmission and reflectance values are 65% and 16% in the wavelength range 400-800nm.

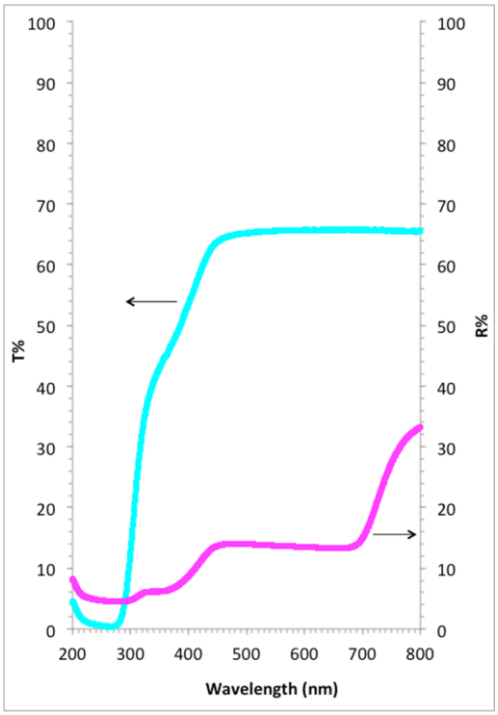


*Fig. 3. Optical transmittance and reflectance spectra of the $In_2O_3$ film.*

The optical band gap corresponding the difference between the minimum of the conduction band and the maximum of the valence band ($E_g$) can be determined from the experimental spectra of the absorption coefficient, $\alpha$, as a function of the photon energy, $h\nu$, using the following equation [18]:

$$(\alpha h\upsilon) = A\left(h\upsilon - E_g\right)^m \quad (2)$$

where m is equal to 1/2 and 2 for direct and indirect transitions, respectively. The graph plot of $(\alpha h\upsilon)^2$ against the photon energy $(h\upsilon)$ for the film is shown in figure 4. Using the above equation, the optical band gap of the film was calculated and given in Fig. 4. The value of the optical band gap is in agreement with those reported in the literature [19, 20].

In order to calculate the refractive index of the film, we recorded transmittance spectra of the films and we calculated the refractive index values of the films using the following equations [21],

$$T = \frac{(1-R)^2 e^{-\alpha d}}{1-R^{-2\alpha d}} \quad (3)$$

where $T$ is the transmittance and $d$ is the thickness of thin film.

$$n = \left(\frac{1+R}{1-R}\right) + \sqrt{\frac{4R}{(1-R)^2} - k^2} \quad (4)$$

where $R$ is the reflectance and $k$ is the extinction coefficient. The refractive index and extinction coefficient dependence of the wavelength are shown in figure 5. As seen Fig. 5, $n$ is

approximately 2.2 between 450nm and 700nm and increases with decreasing the wavelength as a result of normal dispersion. Also, *k* value abruptly increases up to 3.5 at the absorption edge.

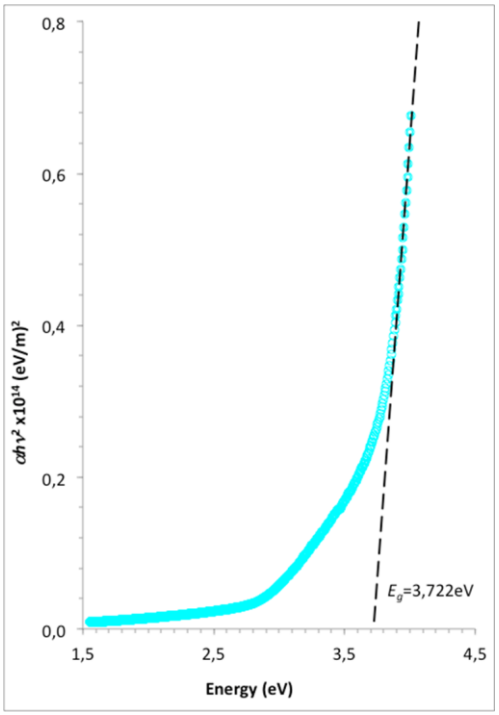


*Fig. 4. Tauc plot of the $In_2O_3$ film.*

The imaginary and real parts of dielectric constant of the film were also determined by the following relations [22].

$$\varepsilon_1 = n^2 - k^2 \quad (5)$$

and

$$\varepsilon_2 = 2nk \quad (6)$$

where $k=\alpha\lambda/4\pi$. The imaginary and real parts of the dielectric constant of the film are respectively shown in Fig. 6. It is seen that while the imaginary part $\varepsilon_1$ increases with increasing wavelength, real part $\varepsilon_2$ decreases and the values of real part are higher than imaginary parts.

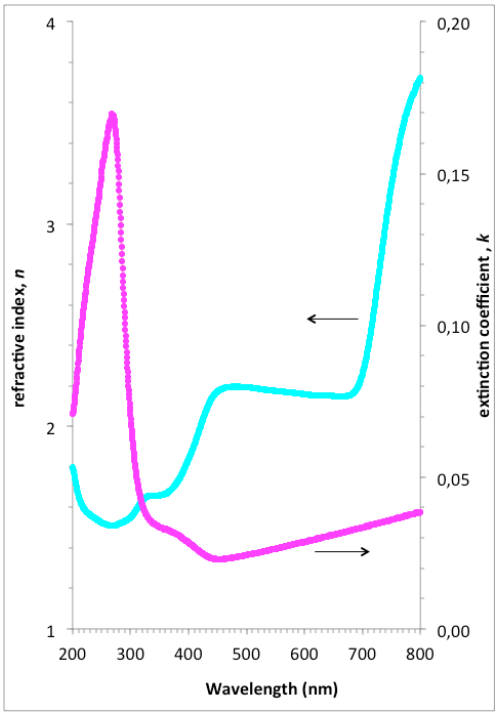


*Fig. 5. The variation of refractive index and extinction coefficient with wavelength for the film*

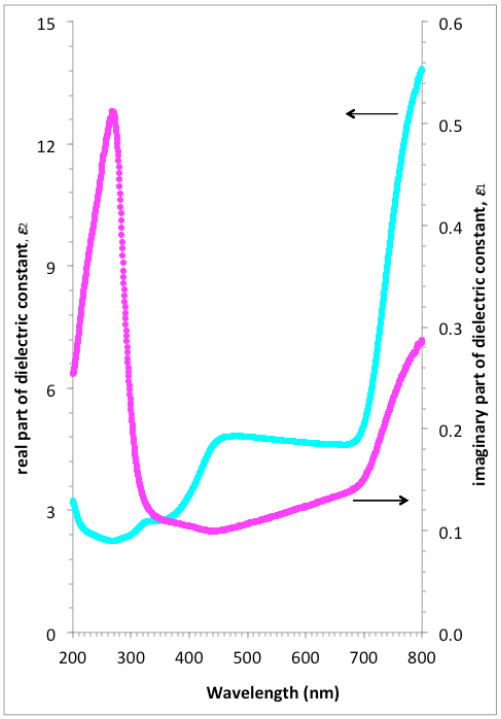


*Fig. 6. The variation of imaginary ($\varepsilon_1$) and real parts ($\varepsilon_2$) of the dielectric constant with wavelength.*

The optical dispersion parameters, $E_o$ (oscillator energy) and $E_d$ (dispersion energy) play an important role in

research of optical materials and optical devices. Therefore, to determine dispersion parameters of the film is very important. The dispersion of the refractive index is discussed in terms of the single-oscillator Wemple–DiDomenico model. The dispersion parameters, which are derived from the refractive index, were evaluated according to the single oscillator model proposed by Wemple and DiDomenico and it is expressed as follows [23]:

$$n^2 - 1 = \frac{E_o E_d}{E_o^2 - E^2} \quad (7)$$

This model describes the dielectric response for transitions below the optical band gap. $(n^2\text{-}1)^{-1}$ vs. $(h\nu)^2$ plots for the $In_2O_3$ film was plotted. $E_o$ and $E_d$ values were determined and found to be 6.848eV and 22.818, respectively. These values obey the single oscillator model. The earlier reported $E_o$ and $E_d$ values of the $In_2O_3$ film are in agreement with values of this study [24, 25].

## 4. Conclusions

The structural, morphological and optical properties of $In_2O_3$ film deposited onto glass substrates by sol gel spin were investigated. XRD result revealed the polycrystalline nature of $In_2O_3$. Pyramid-shaped big crystals were observed on the surface. Optical band gap of $In_2O_3$ was determined as 3.72eV. The refractive index dispersion curve showed that the $In_2O_3$ film obeyed the single oscillator model.

## References

[1] B. G. Svensson, S. J. Pearton and C. Jagadish, Oxide Semiconductors, Elsevier, Amsterdam, 2013.
[2] A. Qurashi, R. Ahsanulhaq, A. Jahangir, T. Yamazaki, Toshinari, Sens. Actuators B. Chem., 221 (2015) 167.
[3] I. Son, B. Lee, C. Kim, S.W. Cho, K. Hyun, J.H. Lee, Liquid Crys. 42 (2015) 1076.
[4] E. Akbarnejad, Z. Ghorannevis, M. Ghorannevis, A. Salar Elahi, Raddiat. Eff. Def. Solids, 170 (2015) 541.
[5] K. Grochowska, S. Katarzyna; K. Siuzdak, Katarzyna; G. Sliwinski, European J. Inorg. Chem. 7 (2015) 1275.
[6] Z. Lin, L. Lan, P. Xiao, S. Sun, Y. Li, w. Song, P. Gao, I. Wang, H. Ning, J. Peng, Appl. Phys. Lett. 107 (2015) 112108.
[7] Y. Hao, G. Meng, C. Ye, L. Zhang Cryst. Growth Des., 5, 1617 (2005).
[8] J. Xu, X. Wang, G. Wang, J. Han, Y.Sun Electrochem. Solid-State Lett., 9 (2006) 103.
[9] S.J. Pearton, F. Ren Nanomater. Nanotechnol., 3, 1 (2013).
[10] Y. Chen, X. Zhou, X. Zhao, X. He, X. Gu Mater. Sci. Eng. B 151, 179 (2008).
[11] A. ElHichou, A. Kachouane, J. L. Bubendorff, M. Addou, J. Ebothe, M. Troyon, A. Bougrine Thin Solid Films 458, 263 (2004).
[12] R.K. Gupta, K. Ghosh, R. Patel, S.R. Mishra, P.K. Kahol Mater. Chem. Phys. 112, 136 (2008).
[13] S. Kaleemulla, A. Sivasankar Reddy, S. Uthanna, P. Sreedhara Reddy Mater. Lett. 61, 4309 (2007).
[14] N.G. Pramod, S.N. Pandey, P.P. Sahay Ceram. International 38 4151–4158 (2012).
[15] Hafeezullah , Zain H. Yamani , Javed Iqbal , Ahsanulhaq Qurashi , Abbas Hakeem J. Alloys Compd. 616 76–80 (2014).
[16] B.D. Cullity, Structure of Polycrystalline Aggregates, 2nd ed., Elements of X-Ray Diffraction, Addison-Wesley Publishing Company, Inc., USA, 1978, p. 284.
[17] Barret CS, Massalski TB. Structure of metals. Oxford: Pergamon Press; 1980.
[18] I. Pankove, Optical Processes in Semiconductors, Prentice-Hall Inc., Englewoord Cliffs, NJ, 1971
[19] L.N. Lau, N.B. Ibrahim, H. Baqiah Applied Surface Science 345 355–359 (2015).
[20] M. Jothibas, C. Manoharan, S. Ramalingam, S. Dhanapandian, M. Bououdina Spectrochim. Acta A 122 171–178 (2014).
[21] F. Abeles (Ed.), Optical Properties of Solids, North-Holland, Publishing Company, London, UK, 1972.
[22] J. N. Hodgson, Optical absorption and dispersion in Solids, Chapman and Hall LTD, 11 New fetter Lane London EC4, 1970.
[23] M. Didomenico, S.H. Wemple, J. Appl. Phys. 40 (1969) 720.
[24] N. Beji, M. Souli, M. Ajili, S. Azzaza, S. Alleg, N. Kamoun Turki, Superlattices Microstruct., 81 (2015) 114-128.
[25] A.P Rambu, D. Sirbu, M. Dobromir, G. G. Rusu, Solid State Sci., 14 (2012) 1543-1549.